BJ www.biochemj.org

BJ Cell

Biochem. J. (2009) **423**, 363–374 (Printed in Great Britain) doi:10.1042/BJ20090666

online data

The NADPH oxidase Nox4 restricts the replicative lifespan of human endothelial cells

Barbara LENER*†[1], Rafał KOZIEŁ*[1], Haymo PIRCHER*, Eveline HÜTTER*, Ruth GREUSSING*, Dietmar HERNDLER-BRANDSTETTER*, Martin HERMANN‡, Hermann UNTERLUGGAUER* and Pidder JANSEN-DÜRR*†[2]

*Institute for Biomedical Aging Research, Austrian Academy of Sciences, Rennweg 10, A-6020 Innsbruck, Austria, †Tyrolean Cancer Research Institute, Innrain 66, A-6020 Innsbruck, Austria, and ‡KMT Laboratory, Department of Visceral, Transplant and Thoracic Surgery, Center of Operative Medicine, Innsbruck Medical University, Innrain 66, A-6020 Innsbruck, Austria

The free radical theory of aging proposes that ROS (reactive oxygen species) are major driving forces of aging, and are also critically involved in cellular senescence. Besides the mitochondrial respiratory chain, alternative sources of ROS have been described that might contribute to cellular senescence. Noxs (NADPH oxidases) are well-known sources of superoxide, which contribute to the antimicrobial capabilities of macrophages, a process involving the prototypical member of the family referred to as Nox2. However, in recent years non-phagocytic homologues of Nox2 have been identified that are involved in processes other than the host defence. Superoxide anions produced by these enzymes are believed to play a major role in signalling by MAPKs (mitogen-activated protein kinases) and stress-activated kinases, but could also contribute to cellular senescence, which is known to involve oxygen radicals. In HUVECs (human umbilical vein endothelial cells), Nox4 is predominantly expressed, but its role in replicative senescence of HUVECs remains to be elucidated. Using shRNA (small-hairpin RNA)-mediated knockdown of Nox4, implicating lentiviral vectors, we addressed the question of whether lifelong depletion of Nox4 in HUVECs would influence the senescent phenotype. We found a significant extension of the replicative lifespan of HUVECs upon knockdown of Nox4. Surprisingly, mean telomere length was significantly reduced in Nox4-depleted cells. Nox4 depletion had no discernable influence on the activity of MAPKs and stress-activated kinases, but reduced the degree of oxidative DNA damage. These results suggest that Nox4 activity increases oxidative damage in HUVECs, leading to loss of replicative potential, which is at least partly independent of telomere attrition.

Key words: DNA damage, human umbilical vein endothelial cell (HUVEC), Nox4, oxidative stress, replicative senescence, telomere attrition.

INTRODUCTION

The free radical theory of aging considers molecular damage caused by the presence and action of ROS (reactive oxygen species) as a major cause of the aging processes in most, if not all, species. The role of ROS as mediators of senescence and determinants of lifespan has been addressed by genetic studies in several model organisms (for a review, see [1]). Thus reducing the level of antioxidant enzymes such as SOD (superoxide dismutase) leads to a consistent reduction of the lifespan in many species, including mouse [2]. Accordingly, extending the antioxidative capacity, for example by overexpression of SOD/catalase [3], has been shown to extend the lifespan in an otherwise short-lived strain of the fruitfly *Drosophila melanogaster*, whereas ectopic overproduction of mitochondrial catalase can prolong the lifespan of mice [4]. However, there are also examples where overexpression of antioxidant enzymes did not extend the lifespan; for example, a large cohort study demonstrated that overexpression of CuZn-SOD does not increase lifespan of the mouse [5]; similarly, catalase-transgenic mice are not long-lived but rather display enhanced sensitivity to oxidative stress [6]. Although these results support the concept that ROS-induced damage contributes to aging processes, at least in some specific genetic backgrounds, the role of the individual antioxidant enzymes in this process remains to be determined.

Concerning human aging, many questions about molecular mechanisms have been addressed using *in vitro* senescence models derived from normal human cells. The proliferative potential of human primary cells in culture is limited, and extended passaging of such cells leads to a state of terminal growth arrest, referred to as replicative senescence. Although the erosion of telomeres, due to insufficient telomerase activity (for a recent review, see [7]), has been recognized as a primary cause of replicative cellular senescence, a variety of other events have been identified that trigger premature senescence. Most notably, oxidative stress was found to induce premature senescence in human fibroblasts [8,9], endothelial cells [10,11] and a variety of other cell types (reviewed in [12]).

The mitochondrial theory of aging [13] suggests a critical role for mitochondrial dysfunction and subsequently increased ROS production as an inducer of aging and premature senescence. Accordingly, replicative senescence of HDFs (human diploid fibroblasts) has been associated with mitochondrial dysfunction, and mitochondrial ROS were identified as important players in the senescence response of HDFs [14–16]. However, mitochondrial dysfunction does not seem to be uniformly responsible for

Abbreviations used: 8-oxo-dG, 8-oxodeoxyguanosine; BrdU, bromodeoxyuridine; DPI, diphenyliodinium; ERK1/2, extracellular-signal-regulated kinase 1/2; FISH, fluorescence *in situ* hybridization; HBSS, Hanks balanced salt solution; HDF, human diploid fibroblast; HUVEC, human umbilical vein endothelial cell; JNK, c-Jun N-terminal kinase; MAPK, mitogen-activated protein kinase; NGS, normal goat serum; Nox, NADPH oxidase; PBGD, porphobilinogen deaminase; PDL, population doubling; PNA, peptide nucleic acid; qPCR, quantitative real-time PCR; RLU, relative light units; ROS, reactive oxygen species; RT, reverse-transcription; SA-β-gal, senescence-associated β-galactosidase; shRNA, small-hairpin RNA; SOD, superoxide dismutase.

[1] These two authors contributed equally to this work

[2] To whom correspondence should be addressed (email p.jansen-duerr@oeaw.ac.at).

senescence in all cell types. In particular, the role of mitochondrial dysfunction in senescence of HUVECs (human umbilical vein endothelial cells) has remained controversial. Depending on the particular strain of HUVEC and the techniques applied to assess mitochondrial function, one can observe a wide range of effects, ranging from serious mitochondrial dysfunction [17] to no effect at all [18], suggesting that other cellular ROS sources may contribute to the senescent phenotype.

Noxs (NADPH oxidases) generate superoxide, which, together with its derivatives, fulfills diverse intracellular functions. Notably, superoxide production by phagocytes and macrophages is activated in response to bacterial or viral infections. This process, characterized by rapid activation of the phagocytic enzyme Nox2 (NADPH oxidase 2), is referred to as 'oxidative burst' [19]. In addition, non-phagocytic members of the Nox gene family have recently been identified. Of those, Nox1 plays a role in host defence (reviewed in [20]), whereas other Nox family members are known to play a role in signal transduction [21]. On the basis of both overexpression and gene-knockdown experiments, it has been shown that Nox1 triggers the activation of JNK (c-Jun N-terminal kinase) by phosphorylation [22]. For Nox4, it has been shown that knockdown leads to decreased MAPK (mitogen-activated protein kinase) activity in various cell types [23,24] and Nox4-induced activation of p38 was shown to drive differentiation of murine cardiomyocytes [25]. Nox4 knockdown in pancreatic cancer cells down-regulated the activity of protein kinase B/Akt [26]. Whereas Nox4 was shown to stimulate the proliferation of various cell types, it was also shown to promote differentiation and restrict cell proliferation ([27–29]; for a recent review, see [30]). Whereas these observations indicate that Nox4 has the potential to modulate the proliferative capacity of various cell types in several ways, the role of NADPH oxidases in replicative senescence of human cells has not been explored so far. Given the implication of Nox4 in ROS production and cellular signalling pathways, we addressed the possibility that Nox4 may be involved in replicative senescence of human endothelial cells.

EXPERIMENTAL

Cell Culture

Endothelial cells of four different donors were isolated from human umbilical veins and maintained in Endothelial Cell Medium (Cambrex BioScience) as described in [10]. To achieve maximal viability, cells were grown on dishes pre-coated with gelatin (Sigma–Aldrich; 0.1 % in Endothelial Cell Medium) [31]. Cells were counted when passaged and PDLs (population doublings) were estimated using the following equation: $n = (\log F - \log I)/0.301$ (n represents the number of population doublings, F the number of cells at the end of one passage and I the number of cells that were seeded at the beginning of one passage). Depending on the donor, cells reached senescence after different numbers of population doublings.

For production of lentiviral particles, HEK-293T cells [human embryonic kidney 293 cells expressing the large T-antigen of SV40 (simian virus 40)] were maintained in DMEM (Dulbecco's modified Eagle's medium) containing 2 mM L-glutamine, 100 units/ml penicillin, 0.1 mg/ml streptomycin and 10 % (w/v) fetal bovine serum (heat-inactivated).

The research has been performed in accordance with the Declaration of Helsinki (2000) of the World Medical Association and has been approved by the Ethics Committee of the Innsbruck Medical University. Consent was obtained from each patient after full explanation of the purpose, nature and risk of all procedures.

Lentiviral infection of HUVEC cells

Production of lentiviral particles was carried out according to the manufacturer's protocol (Addgene) using the packaging plasmids pMD2.G and psPAX2 (both purchased from Addgene) and the lentiviral vector pLKO.1, containing Nox4-specific shRNA (small-hairpin RNA) and control shRNA respectively (Open Biosystems). For lentiviral infection, early passage HUVECs were cultivated in six-well plates. Upon reaching ~70 % confluence, culture medium, containing lentiviral particles to the amount of 2 MOI (multiplicity of infection), was added to the cells in presence of 8 μg/ml hexadimethrine bromide (Sigma–Aldrich), which increases the efficiency of viral infection. At 24 h after infection, medium was changed. Puromycin selection was initiated (500 ng/ml) 48 h post infection.

Staining for SA-β-gal (senescence-associated β-galactosidase)

The senescent status of the cells was monitored by *in situ* staining for SA-β-gal, as described in [10].

PCR-based quantification of mRNA levels

For semiquantitative RT (reverse-transcription)–PCR, total RNAs were isolated from cells using the RNeasy Mini kit (Qiagen). Total RNA (1 μg) was applied to RT using the Transcriptor First Strand cDNA Synthesis Kit (Roche Applied Science) and oligo(dT) primer. Follow-up PCR amplification of Nox4 mRNA was carried out using suitable primers, whereas β-actin served as loading control.

For qPCR (quantitative real-time PCR), primers for the detection of Nox4 mRNA and the housekeepeing gene PBGD (porphobilinogen deaminase) were designed using Primer3 software, as follows: 5′-AGTCCTTCCGTTGGTTTG-3′ (forward) and 5′-AAAGTTTCCACCGAGGAC-3′ (reverse) for Nox4 amplification as well as 5′-CCAGGACATCTTGGATCT-3′ (forward) and 5′-ATGGTAGCCTGCATGGTCTC-3′ (reverse) for PBGD amplification. Total RNA was isolated and used for reverse transcription as previously described in [32]. The cDNA equivalent of 5 ng of RNA was applied to PCR amplification in combination with 15 μl of LightCycler® 480 SYBR Green I Master (Roche Applied Science), a reaction mixture including FastStart Taq DNA Polymerase and SYBR Green I dye for product detection. cDNA concentrations were normalized by the use of the PBGD internal standard. Real-time PCR was performed in triplicate in the LightCycler® 480 Instrument (Roche Applied Science) in a final reaction volume of 50 μl per tube. Cycling conditions were as follows: 95 °C for 8 min (initial denaturation step) followed by 55 cycles of target amplification (95 °C for 15 s, 57 °C for 8 s and 72 °C for 15 s) and final melting (95 °C for 1 min, 60 °C for 30 s, 95 °C continuous with five acquisitions/°C). Crossing points (Ct) for Nox4 and PBGD in control cells/shRNA-treated cells were used for calculation of Nox4 fold expression changes.

Absolute quantification of Nox4 expression in different HUVEC isolates was based on a dilution range of an external plasmid standard to obtain a standard curve (Ct values of the standard versus gene copy numbers). Ct values for Nox4 in HUVEC samples were extrapolated against this plot in order to calculate absolute copy numbers of Nox4 mRNA.

Determination of ROS production by chemiluminescence

ROS were detected by luminol-enhanced chemiluminescence. The assay was performed in 24-well format. Cells were seeded

in order to reach 80–90 % confluency after 24 h. The following day, cells were washed once with HBSS (Hanks balanced salt solution; Sigma–Aldrich). Afterwards, 1.0 ml of HBSS (containing 10 μg/ml luminol and 4 units/ml horseradish peroxidase, both purchased from Sigma–Aldrich) was added to each well. Cells were incubated at 37 °C in a multiple plate reader (HIDEX CHAMELEON, HVD) and ROS production was monitored over a period of 20–25 min by recording light emission (luminescence). DPI (diphenyliodonium; 10 μM; Sigma–Aldrich) was added towards the end of the measurement to abolish Nox-dependent ROS production. The luminescence signal [expressed in RLU (relative light units)] was normalized to cell number.

BrdU (bromodeoxyuridine) staining for quantification of cell proliferation

DNA synthesis was assessed using the 5-bromo-2′-deoxyuridine Labeling and Detection Kit I (Roche Applied Science) according to the manufacturer's recommendations for adherent cells. After the staining procedure, the coverslips were analysed by fluorescence microscopy. Cells of three visual fields were counted and the number of BrdU-positive cells was expressed as a percentage of the total cell number.

Standard immunoblotting analysis

Cellular protein lysates were prepared on ice in RIPA buffer [50 mM NaH_2PO_4/NaH_2PO_4, pH 7.8, 150 mM NaCl, 1 % (v/v) NP-40, 0.5 % Na-based deoxycholate, 0.1 % SDS, 2 mM EDTA, 5 mM NaF and 10 mM $NaVO_4$ and 10 mM β-glycerophosphate] containing protease and phosphatase inhibitors. Lysates were centrifuged (17 500 ***g***, 15 min, 4 °C), and protein concentration in the resulting supernatants was determined using the Detergent Compatible Assay (DC Protein Assay; BioRad). Appropriate amounts of protein were subjected to SDS/PAGE (10 % gels) and transferred to PVDF membranes. Membranes were blocked with 5 % BSA in TBS (50 mM Tris/HCl and 150 mM NaCl)/0.1 % Tween 20 and incubated with primary antibodies overnight. Proteins of interest were detected after incubation with horseradish peroxidase-conjugated secondary antibodies (Dako Cytomation) and visualized with ECL® (enhanced chemiluminescence) reagent (Amersham). Antibodies used were as follows: anti-phospho-ERK1/2 (extracellular-signal-regulated kinase 1/2; New England Biolabs), anti-phospho-JNK (New England Biolabs), anti-phospho-p38 (Cell Signalling), anti-ERK1/2 (Santa Cruz), anti-JNK1 (Santa Cruz), anti-p38 (Cell Signalling) and anti-α-tubulin (Sigma–Aldrich). Results (signal intensities) from three independent experiments were subjected to densitometric analysis using AlphaEaseFC software.

Preparation and fractionation of cell lysates for Nox immunoblotting

Transfected U-2OS cells were scraped off 10-cm-diameter Petri dishes and afterwards re-collected in 900 μl PBS containing protease inhibitors (Roche, Complete, EDTA-free) kept on ice. Cell lysis was achieved by freeze–thaw cycles and sonication. Samples were shock-frozen in liquid nitrogen and quickly thawed to 22 °C. Samples were then sonicated twice for 30 s using a Bianson Sonifier 250 with microtip. During sonication, the microtip was placed in a beaker with ice/water that also contained the sample tubes. After centrifugation (17 500 ***g***, 15 min, 4 °C), the supernatant containing soluble proteins was mixed with standard SDS/PAGE sample buffer and boiled for 5 min. The insoluble pellet was resuspended in membrane protein extraction buffer (20 mM Mops, pH 7.2, 2 % Triton X-100, 0.5 M NaCl and 0.25 M sucrose), sonicated, and centrifuged (17 500 ***g***, 15 min, 4 °C). The supernatant was mixed with an equal volume of membrane protein sample buffer (10 % SDS, 3 % β-mercaptoethanol, 15 % glycerol, 0.025 % bromophenol blue and 75 mM Tris/HCl, pH 7.0) and incubated at 40 °C for 30 min. Soluble and membrane protein fractions were then analysed by SDS-PAGE and subsequent Western blotting. For detection of Nox4, the antibodies anti-Nox4 sc30141 (Santa Cruz Biotechnology) and anti-Nox4 NB110-58849SS (Novus Biologicals) were used. We further applied an affinity-purified goat antiserum obtained against the C-terminal part of Nox4, which was expressed in *Escherichia coli* and purified to homogeneity (H. Pircher, unpublished work).

Analysis of oxidative damage to DNA

Flow-cytometric detection of 8-oxo-dG (8-oxodeoxyguanosine) was as described in [33]. Briefly, the cells were grown to ~90 % confluency on 10-cm-diameter Petri-dishes and were collected (200 ***g***, 5 min) and resuspended in PBS. For fixation, formaldehyde was added to a final concentration of 2.5 % and the cells were incubated for 10 min at 37 °C. Cells were chilled on ice for 1 min, rinsed by centrifugation (200 ***g***, 5 min, 22 °C) and permeabilized by addition of 90 % (v/v) ice-cold methanol. After 30 min incubation on ice, $0.5–1\times10^6$ cells were placed in each assay tube and washed twice with PBS. After centrifugation (800 ***g***, 5 min), cell pellets were blocked for 10 min at room temperature (22 °C) in 300 μl PBS containing 10 % (w/v) NGS (normal goat serum). After two washing steps with PBS containing 0.2 % (w/v) NGS, the cells were stained in 200 μl of avidin-conjugated FITC solution (Sigma, A2050), resuspended 1:200 in PBS and incubated for 1 h at room temperature. After two washings with PBS, cells were resuspended in 400 μl of PBS and analysed by flow cytometry. As a negative control, cells incubated in the absence of avidin-conjugated FITC were used.

Detection of DNA double-strand breaks by γ-H2AX staining

To detect phosphorylation of the histone H2A variant, H2AX, at Ser^{139}, which generates γ-H2AX, a well-established marker of DNA double-strand breaks [34], flow cytometry as well as immunofluorescence procedures were carried out using anti-γ-H2AX antibody (Cell Signaling, #2577), according to the protocols provided by the manufacturer. In both cases, anti-γ-H2AX antibody, diluted 1:50, and a FITC-conjugated swine anti-rabbit Ig secondary antibody (Dako, #F0205), diluted 1:20, were used. As a positive control, cells incubated for 1 h at room temperature with 100 μM H_2O_2 in HBSS were used. As a negative control, cells incubated in the absence of primary antibody were used. Staining of the cells was analysed by confocal microscopy using a microlens-enhanced Nipkow disk-based confocal system UltraVIEW RS (PerkinElmer) mounted on an Olympus IX-70 inverse microscope (Olympus, Nagano, Japan). Images were acquired using a 100× oil immersion objective [Olympus, PlanApo; with a NA (numerical aperture) of 1.4].

Determination of mean telomere length

For flow cytometric analysis of the mean telomere length, a modified protocol based on [35] was used. Briefly, 1×10^6 cells grown on 10-cm-diameter Petri-dishes (to ~90 % confluency) were transferred into FACS tubes and washed once with PBS.

After centrifugation (400 ***g***, 10 min), cells were resuspended in 1 ml of hybridization buffer (49 % formamide, 1 % BSA and 20 mM Tris/HCl, pH 7.2) and rinsed by centrifugation (1000 ***g***, 10 min). The cells were then resuspended in 96.25 of μl hybridization buffer and PNA (peptide nucleic acid) probe (TelC-FITC, Panagene #080506PL-14) was added to a final concentration of 375 nM. After the incubation step (12 min at 85 °C), the tubes were chilled on ice for 2 min and incubated for 90 min at room temperature in the dark. The cells were washed twice with 2 ml of post-hybridization buffer (49 % formamide, 0.1 % BSA, 0.1 % Tween-20, 10 mM Tris/HCl, pH 7.2) and rinsed by centrifugation (1000 ***g***, 10 min). The cells were then washed twice with PBS (1000 ***g***, 10 min) and resuspended in 300 μl of PBS. Cell suspensions were subjected to flow cytometry using a FACSCanto™ II (BD Biosciences). The mean fluorescence intensity (detector FL1) was used to estimate relative telomere length. Human TCL 1301 cells, displaying a relatively constant mean telomere length of roughly 25 kb [35], served as a reference. As a negative control, sample without PNA probe was used.

RESULTS

Expression and activity of NADPH oxidases in young and senescent HUVECs

To determine mRNA levels of NADPH oxidases in young and senescent HUVECs, RNA was prepared from four different HUVEC isolates, which were either harvested at early passage (passage 3) or harvested after extended passaging when cells reached senescence (around passage 25). As described before [32], there is a certain variation in the phenotype between HUVEC strains isolated from different donors. This is also reflected by the fact, that the proliferative capacity of the four different isolates examined, varied between 45 (e.g. HUVEC strain #1) and 55 (e.g. HUVEC strain #3) PDLs before the cultures reached senescence. Data obtained by RNA profiling using Affymetrix™ microarrays indicated that, despite the phenotypical variation noted above, a conserved pattern of gene expression can be observed upon senescence in various HUVEC strains (L. Micutkova, C. Muck and P. Jansen-Dürr, unpublished work). Expression levels of Nox1, 2, 3 and 5 were rather low in young HUVECs and no significant senescence-associated changes in the expression of these genes were observed. However, in all strains a signal for Nox4 was readily detectable by both methods, RT–PCR and qPCR. For all HUVEC strains analysed, the level of Nox4 mRNA was virtually unaltered when young and senescent cultures of HUVECs were compared (Figure 1A, and results not shown). Using RT–PCR, we also detected expression of $p22^{phox}$, the only known additional subunit required for Nox4 activity (reviewed in [36]), in all HUVEC strains (results not shown).

To assess the rate of Nox-derived ROS production, luminol-enhanced chemiluminescence was applied, which is a convenient and sensitive assay to determine cell-associated Nox activity [37]. Using human osteosarcoma cells (U-2OS) stably transfected with expression vectors for both Nox4 and $p22^{phox}$, we confirmed luminol-enhanced chemiluminescence to be a valid method for measuring Nox4-derived ROS, since double-transfected U-2OS cells yielded a robust signal, whereas untransfected U-2OS cells, which lack both enzymatic compounds, yielded no signal in this assay (results not shown). Chemiluminescence signals were quenched more than 90 % upon addition of DPI, further supporting our notion that the assay was specific for detection of Nox activity. Similar results were obtained upon incubation of Nox4-expressing U-2OS cells with the redox-sensitive probe Amplex Red (results not shown), which represents another assay frequently used to detect Nox activity, preferably by measuring extracellular hydrogen peroxide [38].

Significant chemiluminescence signals were detectable in the case of all HUVEC strains at early passage. Signals were efficiently quenched upon the addition of the NADPH oxidase inhibitor DPI (Figure 1B), indicating a significant contribution of NADPH oxidase activity to overall ROS production in HUVEC. Nox activity was also detectable in cells of senescent cultures, although the activity per cell was somewhat lower in senescent cells of all strains (Figure 1B, and results not shown).

Inactivation of Nox4 enhances cell proliferation in HUVECs

To address the growth-modulating potential of Nox4 in HUVECs, we applied lentiviral vectors for delivery of Nox4-specific shRNA. Lentiviral particles are known to efficiently infect HUVECs [32]. Infections were performed in cells of HUVEC strains #1 and #3 at early passage (p5), and cells were grown under puromycin selection to ensure efficient knockdown in all cells. At 42 days after infection, RNA was harvested and analysed by qPCR. This experiment revealed a significant (7–12-fold) down-regulation of Nox4 mRNA in the case of Nox4-specific shRNA, whereas control shRNA showed no effect (Figure 2A).

We also attempted to analyse Nox4-knockdown at the protein level by Western blot analysis, which, due to the limited availability of immunological reagents, has been notoriously difficult (reviewed in [39]). To assess the quality of the immunological reagents available to us, U-2OS osteosarcoma cells were transfected with Nox4 expression vectors. Since Noxs are membrane-bound enzymes, we applied a specific protocol for cell lysis which ensures efficient solubility of membrane proteins that under normal lysis conditions would remain undetectable [40]. As control for the lysis procedure, the related protein Nox5 was used, against which high-quality antibodies (a gift from Professor Karl-Heinz Krause, Department of Pathology and Immunology, University of Geneva, Geneva, Switzerland) have been created. Nox5 was easily detectable in these experiments (Supplementary Figure S1 at http://www.BiochemJ.org/bj/423/bj4230363add.htm), thereby validating our experimental protocol for the detection of Nox enzymes by Western blot analysis. Although a commercially available antibody to Nox4 as well as an affinity-purified goat antiserum directed against the C-terminal part of Nox4 (H. Pircher, unpublished work), detected weak but significant signals in the membrane fraction of Nox4-transfected cells (Supplementary Figure S1), the sensitivity of both antibodies was not sufficient to detect endogenous Nox4 in untransfected HUVECs (results not shown), which precluded the analysis of Nox4-knockdown in HUVECs by Western blot. However, expression of Nox4-specific shRNA led to an almost complete suppression of Nox activity as assessed by luminol-enhanced chemiluminescence (Figure 2B). Chemiluminescence signals were quenched more than 90 % upon addition of DPI (results not shown). Together, these data strongly suggest Nox4 as the functionally relevant Nox isoform in HUVECs.

To determine whether Nox4 depletion affects the rate of cell proliferation, BrdU incorporation studies were performed. As for the parental HUVEC strains, cells derived from strain #3 through infection with control shRNA showed a slightly higher rate of BrdU incorporation (19 ± 3 %; Figure 3A) compared

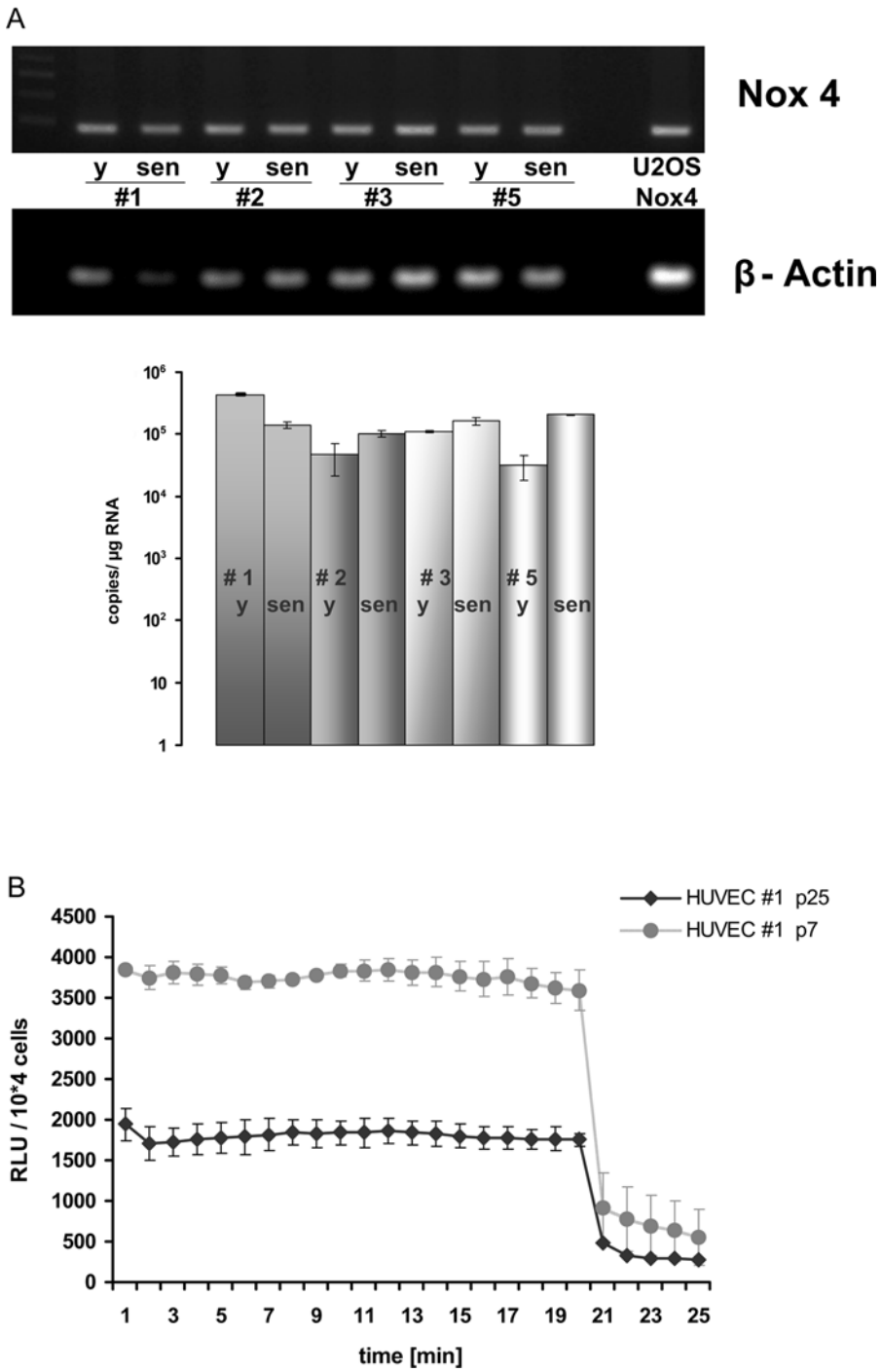

Figure 1 Nox4 expression and activity in young and senescent HUVECs

(**A**) HUVECs from four different donors were grown to senescence. RNA was prepared at early (y) and late (sen) passages and analysed for expression of Nox4 by RT–PCR (upper panel) and qPCR (lower panel). Results are means ± S.D. for three independent experiments. (**B**) Cells of HUVEC strain #1 were analysed for ROS production by measurement of luminol-enhanced chemiluminescence at early passage (passage 7) and at senescence (passage 25), as indicated. At 20 min after onset of the experiment, DPI (10 μM) was added to specifically inhibit Nox activity. Results are means ± S.D. for three independent experiments.

with strain #1 (14 ± 1.5 %; Figure 3A), reflecting the higher proliferative activity of HUVEC strain #3 (results not shown). In both HUVEC strains, expression of Nox4-specific shRNA led to a significant increase in the rate of cell proliferation, as shown by BrdU incorporation (Figure 3A). It is known that Nox4 activity plays an important role in specific signal transduction processes which can modulate cell proliferation, such as signalling through ERK1/2 [24] and stress-activated kinase p38 [25], whereas Nox1 is known to mediate activation of JNK in vascular smooth muscle cells [22]. To investigate whether signalling through these pathways is affected by Nox4 gene knockdown in HUVECs, the expression and activation state of these kinases

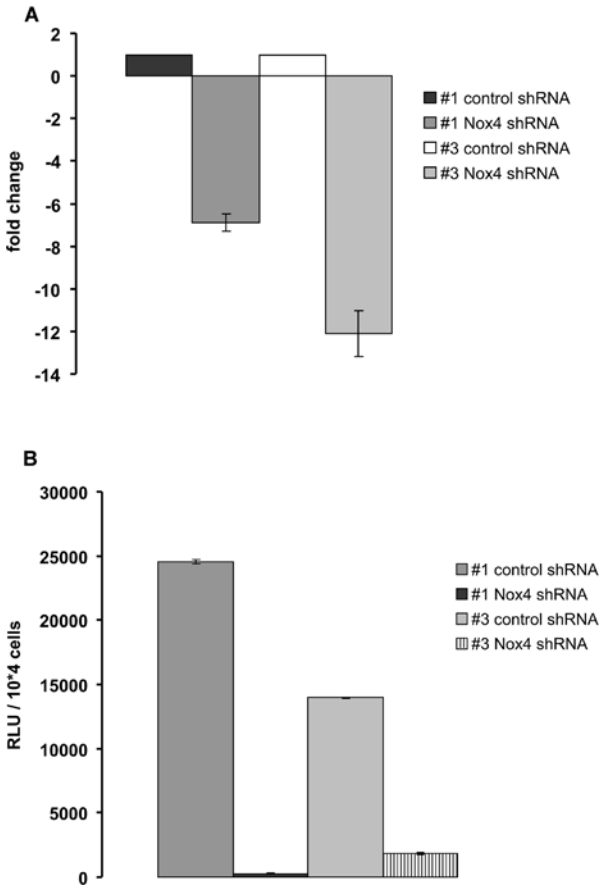

Figure 2 Depletion of Nox4 abrogates ROS production in HUVECs

(**A**) Young HUVECs of strains #1 and #3 were infected with lentiviral particles harbouring control shRNA or Nox4-specific shRNA as indicated. At 42 days after infection, RNA was prepared and Nox4 expression was analysed by qPCR, using PBGD as normalization control. Fold change of Nox4 mRNA level is indicated; shown are the mean results of three independent experiments. (**B**) Validation of Nox4 knockdown by luminol-enhanced chemiluminescence. Cells were grown as described for (**A**) and ROS production was determined by measuring luminol-enhanced chemiluminescence. The relative rate of ROS production is shown, comparing Nox4-knockdown cells and cells expressing control shRNA. Bar graphs represent means ± S.D. of three independent experiments. RLU, relative light unit.

was determined. Extracts were prepared from HUVECs that had either been infected with control shRNA or Nox4-specific shRNA and probed with antibodies to ERK1/2, JNK and p38. To assess the activation status of the respective kinases, we used phosphorylation-specific antibodies directed against phospho-ERK, phospho-JNK and phospho-p38 respectively. Although in control experiments, using human diploid fibroblasts that were either growth-arrested by serum starvation for 72 h or stimulated with 10 % FCS, a clear-cut activation of both ERK and p38 was visible, no significant changes in these signalling pathways could be observed in HUVECs transfected with Nox4-specific shRNA. Similarly, control experiments with anisomycin-treated human fibroblasts revealed a clear increase in the levels of phosphorylated JNK, whereas the levels of both JNK and phospho-JNK were not significantly affected by Nox4 shRNA (Figure 3B). Together, these data suggest that down-regulation of Nox4 in two independent HUVEC isolates did not significantly affect the activity of the three protein kinases studied (Figure 3C).

Inactivation of Nox4 delays HUVEC replicative senescence

To study the role of Nox4 in replicative senescence of HUVEC, early passage cells of both strains #1 and #3 were subjected to lentiviral infection, with particles harbouring control shRNA or Nox4-specific shRNA, and grown to senescence. Efficient and persistent knockdown of Nox4 was confirmed by qPCR (Figure 4A) and luminol-enhanced chemiluminescence (results not shown). Cell proliferation was assessed by cell counting at every passage, thereby cPDLs (cumulated PDLs) were calculated. We found that shRNA-mediated knockdown of Nox4 led to a significant extension of the population doubling capacity in both HUVEC strains #1 (Figure 4B) and #3 (Figure 4C). Accordingly, the relative proportion of cells that stained positive for SA-β-gal activity was significantly reduced upon transfection with Nox4-specific shRNA (Figure 4D).

Replicative senescence is known to be triggered primarily by telomere shortening (for a recent review, see [7]), although it is known that other processes, such as oxidative stress, can shorten the cellular lifespan as well [10,11,41]. To elucidate the role of telomere shortening in context with the observed lifespan extension in response to Nox4 depletion, telomere length was determined in Nox4-depleted cells as well as in control cells. Telomere length was estimated by flow FISH (fluorescence *in situ* hybridization) [42], using telomeres of a stable T-cell line as size markers [35]. The mean telomere length of HUVECs was gradually reduced through extended passaging to a minimal length of roughly 20 kb when cells reached senescence (results not shown; see also [43]). This finding is in agreement with the observations of others who reported telomere shortening to be a key mechanism of cellular senescence in HUVECs [11]. When the influence of Nox4 knockdown on mean telomere length was analysed, we found that the mean telomere length of 22 kb in control cells of strain #3 at passage 15 was reduced to 13 kb in the case of Nox4-depleted cells of the same strain. Similarly, telomere length of 28 kb in control cells of strain #1 at passage 17 was reduced to 18 kb in Nox4-depleted cells of the same strain (Figure 5). These findings suggest that depletion of Nox4 extends the proliferative capacity of HUVECs, resulting in a decreased mean telomere length in Nox4-depleted cells.

Inactivation of Nox4 delays the accumulation of oxidative damage

The results obtained so far suggest that Nox4 contributes to replicative senescence of HUVECs. ROS-induced damage to nucleic acids (reviewed in [16]) and proteins [44] is believed to contribute to cellular senescence, and our results raise the possibility that, in HUVECs, ROS produced by Nox4 may be involved in this process. Accordingly, the observed delay of senescence in Nox4-deficient HUVECs may be due to reduced oxidative damage otherwise affecting cellular constituents such as DNA and proteins. To test this hypothesis, the degree of DNA damage was determined by quantification of 8-oxo-dG, an established marker of oxidative DNA damage [33]. To this end, HUVEC strains #1 and #3, infected with either control shRNA or Nox4-specific shRNA, were stained with avidin-FITC, a well-established and specific ligand for 8-oxo-dG [33]. Fluorescence intensities were analysed by flow cytometry. This experiment revealed a significant reduction of 8-oxo-dG content in Nox4-knockdown cells (Figure 6A).

To further characterize Nox4-derived DNA damage, cells were stained with antibodies to γ-H2AX and analysed by indirect immunofluorescence. The histone variant H2AX is phosphorylated in response to DNA double-strand breaks to yield

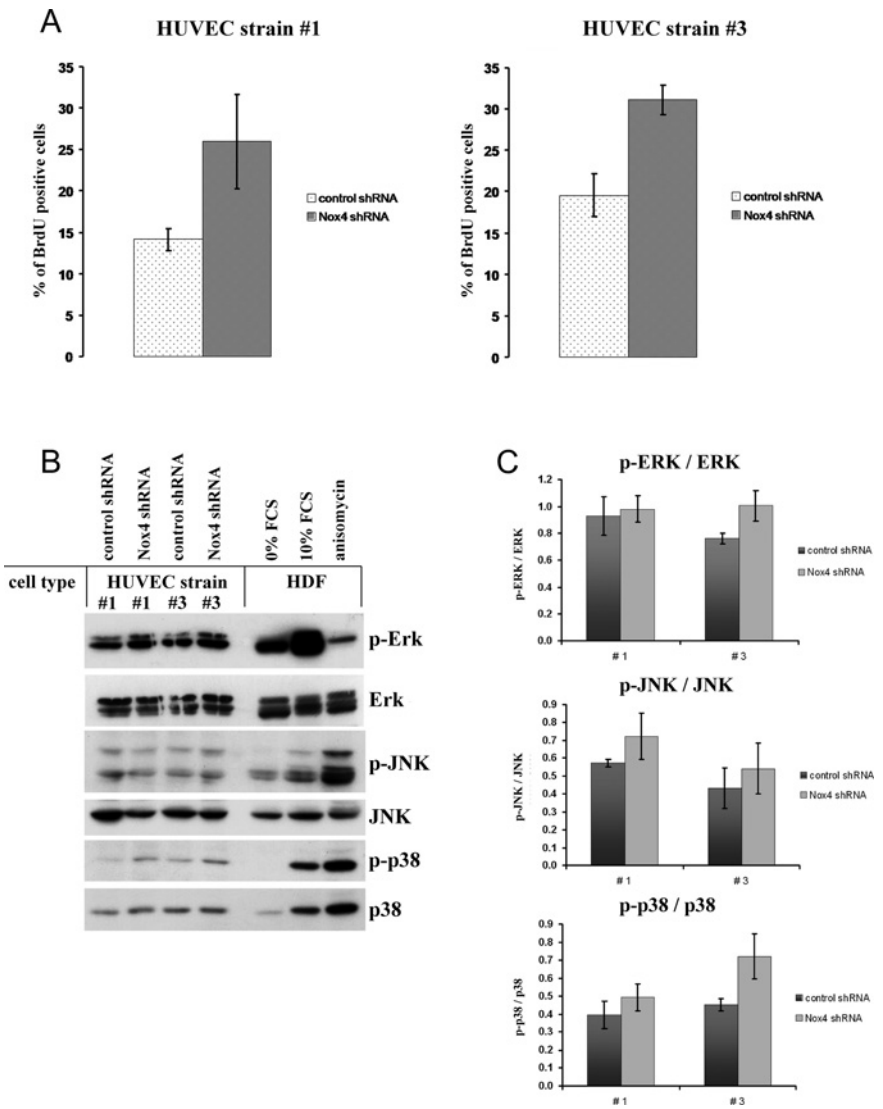

Figure 3 Depletion of Nox4 enhances cell proliferation

(**A**) Young HUVECs of strain #1 and #3 were infected with lentiviral particles harbouring control shRNA or Nox4-specific shRNA. At 42 days after infection, the proliferation rate was determined by BrdU incorporation experiments. The number of BrdU-positive cells was assessed as described in the Experimental section. The results are separately depicted for HUVEC strains #1 and #3; each case is representative of three independent experiments. (**B**) Cells of HUVEC strains #1 and #3 were treated as described for (**A**). At 42 days after infection, cells were harvested. Cellular extracts were subjected to SDS/PAGE and analysed by Western blot analysis using antibodies to ERK, phospho-ERK, JNK, phospho-JNK, p38 and phospho-p38, as indicated. The quality of phospho-antibodies was evaluated using extracts of human fibroblasts that were either serum-starved for 72 h, stimulated with 10% FCS (10 min), or treated with anisomycin (100 nM, 20 min) respectively. Expression levels and phosphorylation status of ERK, JNK and p38 were analysed in three independent experiments; shown here are the results from one representative experiment. (**C**) Results from three independent experiments, as described in (**B**), were evaluated by densitometric and statistical analysis. The signal for phosphorylated protein was normalized to the signal intensity of the corresponding unphosphorylated form. Results are means $\pm$ S.E.M. for HUVEC strains #1 and #3, as indicated.

γ-H2AX, which is recruited to sites of DNA damage [34]. We detected specific nuclear γ-H2AX staining in control cells (transfected with control shRNA), which was markedly reduced in Nox4-depleted cells (Figure 6B). In both cell types, γ-H2AX staining was enhanced upon treatment with H_2O_2, providing a control for the staining assay. γ-H2AX staining intensity was quantified using flow cytometry (Figure 6C), which confirmed significantly reduced fluorescence in Nox4-depleted cells. DNA damage is known to initiate antiproliferative signals and contribute to senescence in several models of senescence *in vitro* (reviewed in [45]) and probably also *in vivo* (reviewed in [46]). Together, these results suggest that Nox4-derived ROS induce DNA damage in HUVECs, thereby leading to the establishment of cellular senescence.

DISCUSSION

The occurrence of ROS, originating from the mitochondrial electron transport chain, is up-regulated with age in many species, including humans, and solid evidence suggests that mitochondria-derived ROS mechanistically contribute to aging in a variety of experimental model systems. Concerning the *in vitro* senescence of human diploid fibroblasts, it has been

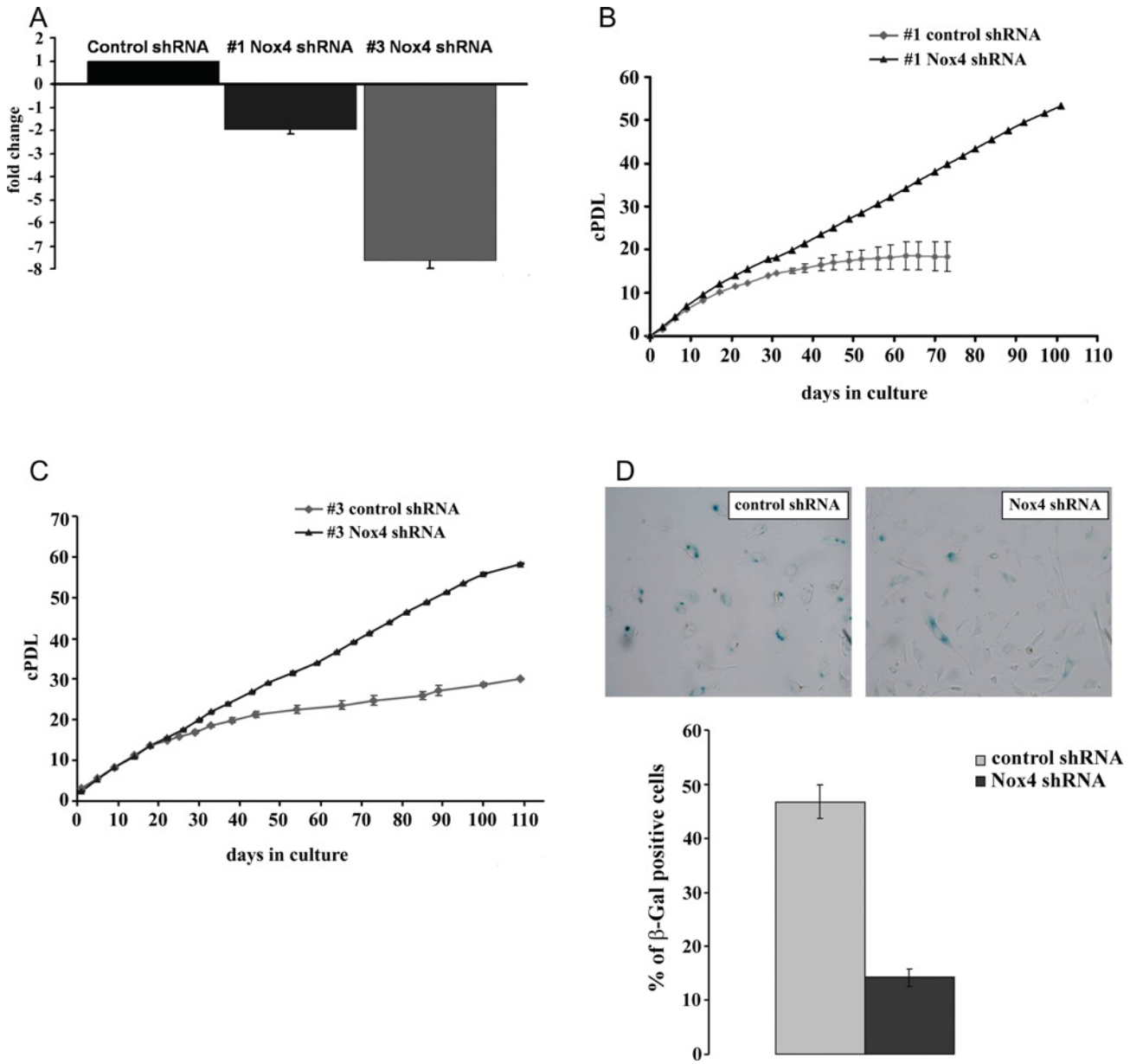

Figure 4 Depletion of Nox4 delays the onset of replicative senescence

(**A**) Cells of HUVEC strains #1 and #3 were infected with lentiviral particles, harbouring either control shRNA or Nox4-specific shRNA. RNA was prepared 110 days after infection (for strain #3) and 30 days after infection (for strain #1) respectively. The expression level of Nox4 was determined by qPCR. The fold regulation of Nox4 is shown in either case; results are means ± S.D. for three independent experiments. (**B**) Cells of HUVEC strain #1 were treated as described for (**A**) and grown for 100 days after infection. Cells were passaged at regular intervals and thereby counted. Cell numbers were used to establish a growth curve, displaying cumulated population doublings. Cells were counted in three independent parallel experiments. S.D. values are indicated by error bars. (**C**) Cells of HUVEC strain #3 were treated as described for (**A**) and grown for 110 days after infection. Cells were passaged at regular intervals and counted. Cell numbers were used to establish a growth curve, displaying cumulative population doublings. Cells were counted in three independent parallel experiments. S.D. values are indicated by error bars. (**D**) At 110 days post-infection, cells of HUVEC strain #3 (treated as described for **A**) were stained for presence of SA-β-gal activity. Bars indicate the relative percentage of β-gal-positive cells (±S.D.); results; are the means derived from three independent experiments.

demonstrated that mitochondrial dysfunction and increased ROS production are tightly linked in senescent cells, and it is now widely accepted that dysfunctional mitochondria play a key role in fibroblast senescence. Concerning human endothelial cells, the link between senescence and mitochondrial dysfunction is less clear, raising the possibility that other ROS sources could contribute to senescence of human endothelial cells. To address the question of whether Noxs play a role in the senescence response of HUVECs, we have analysed the expression pattern of Nox genes in HUVECs isolated from four different donors. PCR analysis revealed consistent expression of Nox4 in all four isolates, whereas the expression level of other Nox family members was rather low. To assess the influence of Nox4 on the replicative potential of these cells, shRNA-encoding vectors were used for sustained depletion of Nox4 in HUVEC. Nox4 knockdown enhanced the rate of cell proliferation and resulted in a significant extension of cellular lifespan, consistent with the model that Nox4-derived ROS contribute

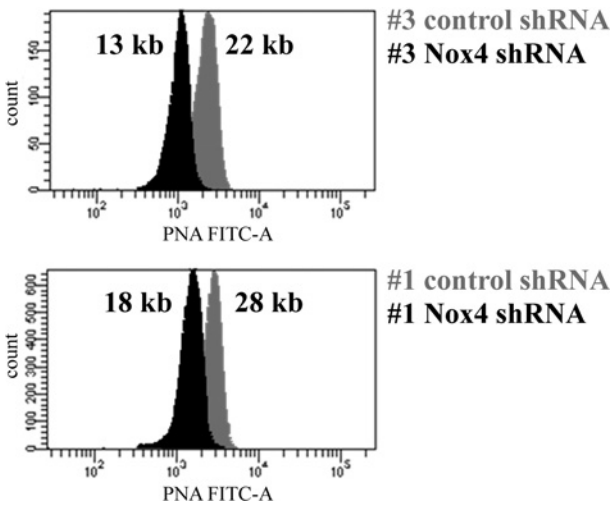

Figure 5 Depletion of Nox4 enhances telomere shortening

Cells of HUVEC strains #1 and #3 infected with lentiviral particles, harbouring either control shRNA or Nox4-specific shRNA, were analysed at passage 17 (HUVEC strain #1) or at passage 15 (HUVEC strain #3), as indicated. Telomere length was determined by the flow FISH technique as described in the Experimental section, using telomeres of TCL 1301 cells as a size marker. In each case, the calculated mean telomere length is indicated.

to the onset of replicative senescence in human endothelial cells.

Role of Nox enzymes in signal transduction and cell proliferation in HUVECs

RT–PCR analysis revealed Nox4 to be the major NADPH oxidase isoform in four different HUVEC isolates. In contrast with findings reported by others [47], Nox2 was detectable neither at the mRNA level nor at the protein level in the HUVEC strains implicated in this study. Similarly, mRNA levels for Nox1, Nox3, and Nox5 were rather low in all four HUVEC isolates (B. Lener, unpublished work). Limitations concerning the sensitivity of available antibodies restricts reliable detection of Nox4 protein to cells with high expression levels (Supplementary Figure S1). None of the available antibodies was able to detect endogenous Nox4 protein in HUVECs (results not shown). In the light of this, we chose to assess cellular ROS production to determine the efficiency of shRNA-mediated Nox4 depletion. Using U-2OS cells stably transfected with both Nox4 and $p22^{phox}$ expression vectors, luminol-enhanced chemiluminescence was established as a convenient method to assess Nox4 activity in cells. Using this assay, we found the presence of Nox4 mRNA is closely connected with the presence of elevated ROS production, which could be successfully inhibited by the Nox inhibitor DPI. DPI-sensitive ROS production was lost upon shRNA-mediated knockdown of Nox4, supporting our conclusion that the majority of Nox activity in HUVEC is due to Nox4.

We found that shRNA-mediated abrogation of Nox4 activity results in increased cellular proliferation. Nox4 is required for proliferation of various cell types [27–29]; on the other hand, Nox4 can also promote differentiation and restrict cell proliferation (reviewed in [30]). These observations indicate that the influence of Nox4 on cell proliferation capacity is cell-type specific and may be further influenced by cell culture conditions. On the basis of the literature [48,49], one would expect that inactivation of Nox4 reduces signalling through ERK1/2 and/or stress-activated kinase pathways. However, we failed to detect any significant decrease in ERK phosphorylation, JNK phosphorylation and p38 kinase phosphorylation, suggesting that the maintenance of those pathways may require relatively low levels of Nox4 activity in HUVECs.

Oxidative stress and cellular senescence: the role of mitochondria and alternative ROS sources

Employing high-resolution respirometry, we have previously shown that mitochondria are partially uncoupled in senescent human dermal fibroblasts [14] and that experimental uncoupling of mitochondria in young fibroblasts induces premature senescence [15]. In a similar study, mitochondrial dysfunction was observed in senescent human lung fibroblasts, and mitochondrial ROS production was identified as one of the causes of replicative senescence in human fibroblasts [16]. A significant increase in oxidative stress was also observed in senescent human endothelial cells [10,11]; however, the sources for increased ROS production have remained elusive. Depending on the particular strain of HUVEC and the techniques used to assess mitochondrial function, one can observe a wide range of effects, ranging from serious mitochondrial dysfunction [17] to no effect at all [18]. Whereas more work will be required to establish the role of mitochondrial dysfunction in HUVEC senescence, the results obtained in the present study indicate that ROS derived from Nox4 plays an important role in HUVEC replicative senescence. Lifespan extension linked to Nox4 knockdown could not been observed upon the application of protocols implicating short-term knockdown, via transient transfection with Dharmacon oligonucleotides (H. Pircher, unpublished work). The occurrence of the effects described requires lifelong depletion of Nox4, which can only be obtained using lentiviral vectors. We think that the influence of Nox4 activity on lifespan is based on a continuous accumulation of ROS and oxidative damage, already starting at early passage. In this respect, it is conceivable that Nox4-derived ROS, in addition to their role as signalling molecules, induce damage to cellular constituents such as DNA and proteins. This idea is supported by our finding that knockdown of Nox4 resulted in a drastic reduction of DNA damage (Figure 6), which was accompanied by reduced levels of protein damage, determined as protein carbonyl groups (results not shown). This finding suggests that ROS produced by Nox4 may contribute to lifespan restriction caused by accumulation of damaged DNA (and proteins).

Surprisingly, HUVECs infected with control shRNA underwent senescence-associated growth arrest with relatively high mean telomere length (roughly 20 kb; R. Kozieł, unpublished work), whereas Nox4-depleted HUVECs were still proliferating with significantly shorter telomeres (e.g. 13 kb in HUVEC strain #3, see Figure 5), suggesting that growth arrest in normal HUVECs may be at least in part telomere-independent. Others have shown that overexpression of Nox4 results in the induction of a senescence-like growth arrest in immortalized murine fibroblasts [50], and that angiotensin II accelerates the onset of senescence in endothelial progenitor cells [51], probably by stimulating Nox2 activity [52]. Whereas overexpression of a foreign gene in an immortalized cell line does not necessarily reveal the physiological role of the gene in question, the approach chosen by us, namely to deplete cells of endogenous Nox4, seems more suitable to reveal its physiological function. During the preparation of the present manuscript, Schilder et al. [53] reported that chronic incubation of HUVECs with the plant-derived polyphenol resveratrol induces a senescence-like phenotype. They showed further that inhibition of cell cycle progression in resveratrol-treated cells could be alleviated by

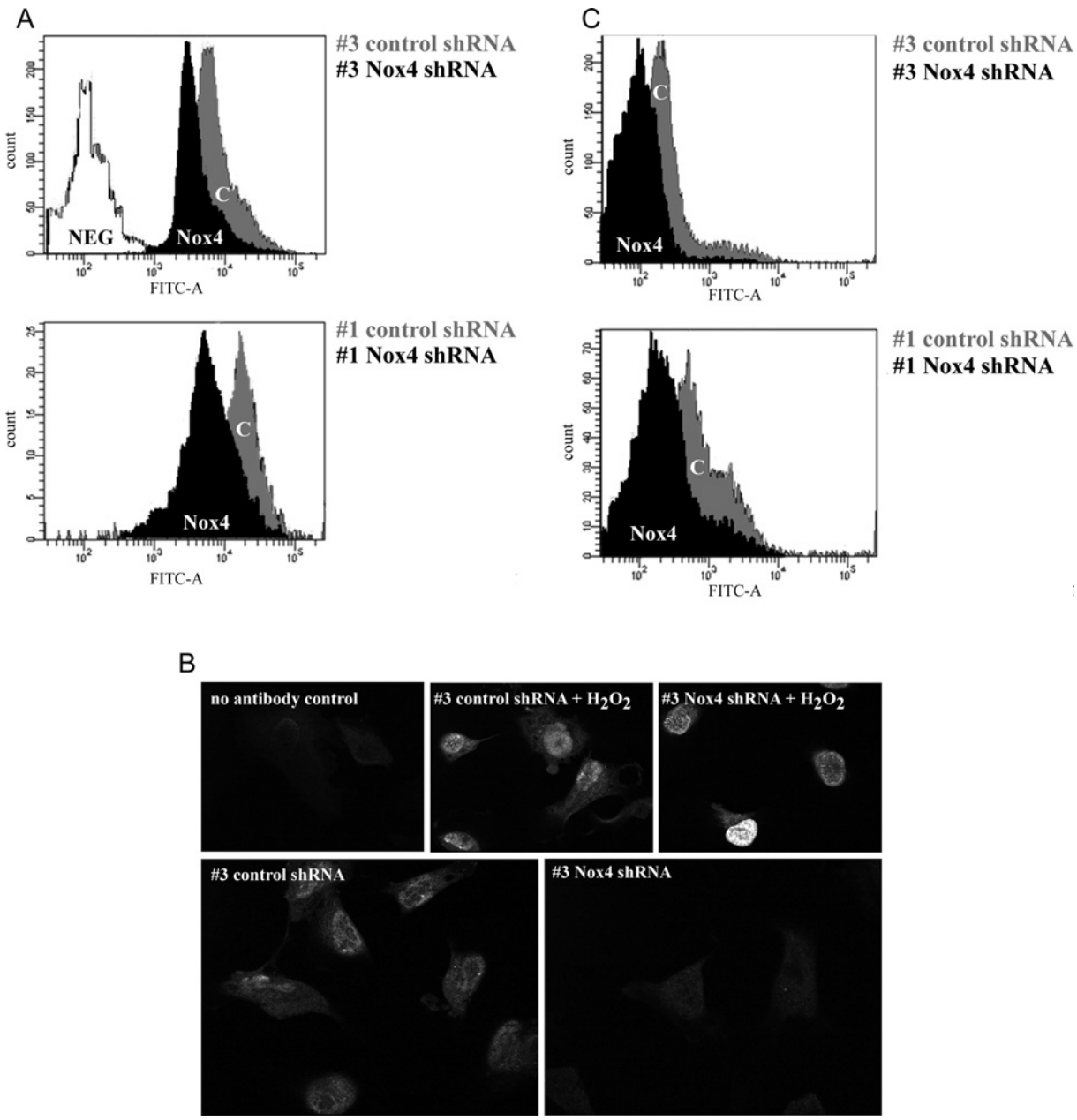

Figure 6 Depletion of Nox4 prevents DNA damage

The degree of DNA damage was determined by quantification of 8-oxo-dG (**A**) and histone variant γ-H2AX (**B** and **C**). (**A**) Cells of HUVEC strains #1 and #3 (p5) were infected with lentiviral particles harbouring control shRNA and Nox4-specific shRNA respectively. At passage 23 (strain #1) or passage 22 (strain #3), cells were stained with avidin–FITC. Fluorescence intensity was analysed by flow cytometry. As a negative control, cells incubated in the absence of avidin-conjugated FITC were used. (**B**) HUVEC strain #3 was infected with control shRNA or Nox4-specific shRNA at passage 5. At passage 26, cells were stained using indirect immunofluorescence and anti-γ-H2AX primary antibody. Cells incubated for 1 h at room temperature with 100 μM H_2O_2 in HBSS were used as positive control. As negative control, primary antibody was omitted. Samples were analysed using confocal microscopy. (**C**) HUVEC strains #1 and #3 (p5) were infected with either control shRNA or Nox4-specific shRNA, and stained as described in (**B**). Staining was performed at passage 23 (strain #1) and passage 22 (strain #3), respectively. Shown here is the histogram of one representative experiment ($n = 3$).

knocking down Nox1 in short-term transient transfections with shRNA; a similar albeit weaker effect was also observed upon shRNA-mediated knockdown of Nox4. Schilder et al. [53] showed that depletion of either Nox4 or Nox1 had no effects on the phenotype of wild-type HUVECs in the absence of resveratrol. It is conceivable that this observation, which contrasts with our present finding that Nox4 knockdown significantly extends HUVEC lifespan, reflects inefficient knockdown of Nox4 achievable by transient transfection. Therefore the present study, applying lifelong Nox4 depletion in HUVECs in the absence of any pharmacological treatment, demonstrates for the first time that replicative senescence of human endothelial cells can be delayed by reducing endogenous Nox4 activity. Preliminary data from our laboratory suggest that Nox4 knockdown also leads to a moderate lifespan extension in human fibroblasts (R. Greussing and P. Jansen-Dürr, unpublished work), suggesting a more general role of Nox4 in cellular senescence; however, further work will be required to clarify this point.

AUTHOR CONTRIBUTION

Barbara Lener and Rafał Kozieł designed the experiments and carried out the majority of the experiments. Haymo Pircher set up the Western blot conditions and performed Nox4/5 Western blots. Eveline Hütter helped with the measurements of ROS production. Ruth Greussing prepared lentiviral vectors and performed Nox4-knockdown in fibroblasts. Dietmar Herndler-Brandstetter helped with the analysis of telomere size. Martin Hermann performed confocal microscopy. Hermann Unterluggauer performed protein carbonyl analysis. Pidder Jansen-Dürr designed the experiments and wrote the paper.

ACKNOWLEDGEMENT

We acknowledge excellent technical support by Michael Neuhaus.

FUNDING

This work was supported by grants from the Austrian Science Funds [grant number NFN S93] and the European Union (Integrated Project MiMage) [grant number LSHM-CT-2004-512020].

REFERENCES

1 Sohal, R. S., Mockett, R. J. and Orr, W. C. (2002) Mechanisms of aging: an appraisal of the oxidative stress hypothesis. Free Radical Biol. Med. **33**, 575–586
2 Kokoszka, J. E., Coskun, P., Esposito, L. A. and Wallace, D. C. (2001) Increased mitochondrial oxidative stress in the $Sod2^{+/-}$ mouse results in the age-related decline of mitochondrial function culminating in increased apoptosis. Proc. Natl. Acad. Sci. U.S.A. **98**, 2278–2283
3 Orr, W. C. and Sohal, R. S. (1994) Extension of life-span by overexpression of superoxide dismutase and catalase in *Drosophila melanogaster*. Science **263**, 1128–1130
4 Schriner, S. E., Linford, N. J., Martin, G. M., Treuting, P., Ogburn, C. E., Emond, M., Coskun, P. E., Ladiges, W., Wolf, N., Van Remmen, H. et al. (2005) Extension of murine life span by overexpression of catalase targeted to mitochondria. Science **308**, 1909–1911
5 Huang, T. T., Carlson, E. J., Gillespie, A. M., Shi, Y. and Epstein, C. J. (2000) Ubiquitous overexpression of CuZn superoxide dismutase does not extend life span in mice. J. Gerontol. A Biol. Sci. Med. Sci. **55**, B5–9
6 Chen, X., Liang, H., Van Remmen, H., Vijg, J. and Richardson, A. (2004) Catalase transgenic mice: characterization and sensitivity to oxidative stress. Arch. Biochem. Biophys. **422**, 197–210
7 Shawi, M. and Autexier, C. (2008) Telomerase, senescence and ageing. Mech. Ageing Dev. **129**, 3–10
8 Chen, Q. and Ames, B. N. (1994) Senescence-like growth arrest induced by hydrogen peroxide in human diploid fibroblast F65 cells. Proc. Natl. Acad. Sci. U.S.A. **91**, 4130–4134.
9 von Zglinicki, T., Saretzki, G., Docke, W. and Lotze, C. (1995) Mild hyperoxia shortens telomeres and inhibits proliferation of fibroblasts: a model for senescence? Exp. Cell Res. **220**, 186–193.
10 Unterluggauer, H., Hampel, B., Zwerschke, W. and Jansen-Durr, P. (2003) Senescence-associated cell death of human endothelial cells: the role of oxidative stress. Exp. Gerontol. **38**, 1149–1160
11 Kurz, D. J., Decary, S., Hong, Y., Trivier, E., Akhmedov, A. and Erusalimsky, J. D. (2004) Chronic oxidative stress compromises telomere integrity and accelerates the onset of senescence in human endothelial cells. J. Cell Sci. **117**, 2417–2426
12 Colavitti, R. and Finkel, T. (2005) Reactive oxygen species as mediators of cellular senescence. IUBMB Life **57**, 277–281
13 Miquel, J. (1991) An integrated theory of aging as the result of mitochondrial-DNA mutation in differentiated cells. Arch. Gerontol. Geriatr. **12**, 99–117
14 Hutter, E., Renner, K., Pfister, G., Stockl, P., Jansen-Dürr, P. and Gnaiger, E. (2004) Senescence-associated changes in respiration and oxidative phosphorylation in primary human fibroblasts. Biochem. J. **380**, 919–928
15 Stockl, P., Zankl, C., Hutter, E., Unterluggauer, H., Laun, P., Heeren, G., Bogengruber, E., Herndler-Brandstetter, D., Breitenbach, M. and Jansen-Durr, P. (2007) Partial uncoupling of oxidative phosphorylation induces premature senescence in human fibroblasts and yeast mother cells. Free Radical Biol. Med. **43**, 947–958
16 Passos, J. F., Saretzki, G., Ahmed, S., Nelson, G., Richter, T., Peters, H., Wappler, I., Birket, M. J., Harold, G., Schaeuble, K. et al. (2007) Mitochondrial dysfunction accounts for the stochastic heterogeneity in telomere-dependent senescence. PLoS Biol. **5**, e110
17 Jendrach, M., Pohl, S., Voth, M., Kowald, A., Hammerstein, P. and Bereiter-Hahn, J. (2005) Morpho-dynamic changes of mitochondria during ageing of human endothelial cells. Mech. Ageing Dev. **126**, 813–821
18 Hutter, E., Unterluggauer, H., Garedew, A., Jansen-Durr, P. and Gnaiger, E. (2006) High-resolution respirometry – a modern tool in aging research. Exp. Gerontol. **41**, 103–109
19 Babior, B. M., Lambeth, J. D. and Nauseef, W. (2002) The neutrophil NADPH oxidase. Arch. Biochem. Biophys. **397**, 342–344
20 Krause, K. H. (2004) Tissue distribution and putative physiological function of NOX family NADPH oxidases. Jpn. J. Infect. Dis. **57**, S28–S29
21 Torres, M. and Forman, H. J. (2003) Redox signaling and the MAP kinase pathways. Biofactors **17**, 287–296
22 Schroder, K., Helmcke, I., Palfi, K., Krause, K. H., Busse, R. and Brandes, R. P. (2007) Nox1 mediates basic fibroblast growth factor-induced migration of vascular smooth muscle cells. Arterioscler. Thromb. Vasc. Biol. **27**, 1736–1743
23 Brandes, R. P. (2003) Role of NADPH oxidases in the control of vascular gene expression. Antioxid. Redox Signal. **5**, 803–811
24 Gorin, Y., Ricono, J. M., Wagner, B., Kim, N. H., Bhandari, B., Choudhury, G. G. and Abboud, H. E. (2004) Angiotensin II-induced ERK1/ERK2 activation and protein synthesis are redox-dependent in glomerular mesangial cells. Biochem. J. **381**, 231–239
25 Li, J., Stouffs, M., Serrander, L., Banfi, B., Bettiol, E., Charnay, Y., Steger, K., Krause, K. H. and Jaconi, M. E. (2006) The NADPH oxidase NOX4 drives cardiac differentiation: role in regulating cardiac transcription factors and MAP kinase activation. Mol. Biol. Cell **17**, 3978–3988
26 Mochizuki, T., Furuta, S., Mitsushita, J., Shang, W. H., Ito, M., Yokoo, Y., Yamaura, M., Ishizone, S., Nakayama, J., Konagai, A. et al. (2006) Inhibition of NADPH oxidase 4 activates apoptosis via the AKT/apoptosis signal-regulating kinase 1 pathway in pancreatic cancer PANC-1 cells. Oncogene **25**, 3699–3707
27 Petry, A., Djordjevic, T., Weitnauer, M., Kietzmann, T., Hess, J. and Gorlach, A. (2006) NOX2 and NOX4 mediate proliferative response in endothelial cells. Antioxid. Redox Signal. **8**, 1473–1484
28 Li, S., Tabar, S. S., Malec, V., Eul, B. G., Klepetko, W., Weissmann, N., Grimminger, F., Seeger, W., Rose, F. and Hanze, J. (2008) NOX4 regulates ROS levels under normoxic and hypoxic conditions, triggers proliferation, and inhibits apoptosis in pulmonary artery adventitial fibroblasts. Antioxid. Redox Signal. **10**, 1687–1698
29 Mofarrahi, M., Brandes, R. P., Gorlach, A., Hanze, J., Terada, L. S., Quinn, M. T., Mayaki, D., Petrof, B. and Hussain, S. N. (2008) Regulation of proliferation of skeletal muscle precursor cells by NADPH oxidase. Antioxid. Redox Signal. **10**, 559–574
30 Brandes, R. P. and Schroder, K. (2008) Composition and functions of vascular nicotinamide adenine dinucleotide phosphate oxidases. Trends Cardiovasc. Med. **18**, 15–19
31 Unterluggauer, H., Hutter, E., Voglauer, R., Grillari, J., Voth, M., Bereiter-Hahn, J., Jansen-Durr, P. and Jendrach, M. (2007) Identification of cultivation-independent markers of human endothelial cell senescence *in vitro*. Biogerontology **8**, 383–397
32 Muck, C., Micutkova, L., Zwerschke, W. and Jansen-Durr, P. (2008) Role of insulin-like growth factor binding protein-3 in human umbilical vein endothelial cell senescence. Rejuvenation Res. **11**, 449–453
33 Struthers, L., Patel, R., Clark, J. and Thomas, S. (1998) Direct detection of 8-oxodeoxyguanosine and 8-oxoguanine by avidin and its analogues. Anal. Biochem. **255**, 20–31
34 Kinner, A., Wu, W., Staudt, C. and Iliakis, G. (2008) γ-H2AX in recognition and signaling of DNA double-strand breaks in the context of chromatin. Nucleic Acids Res. **36**, 5678–5694
35 Fehrer, C., Voglauer, R., Wieser, M., Pfister, G., Brunauer, R., Cioca, D., Grubeck-Loebenstein, B. and Lepperdinger, G. (2006) Techniques in gerontology: cell lines as standards for telomere length and telomerase activity assessment. Exp. Gerontol. **41**, 648–651
36 Kawahara, T., Ritsick, D., Cheng, G. and Lambeth, J. D. (2005) Point mutations in the proline-rich region of $p22^{phox}$ are dominant inhibitors of Nox1- and Nox2-dependent reactive oxygen generation. J. Biol. Chem. **280**, 31859–31869
37 Rinaldi, M., Moroni, P., Paape, M. J. and Bannerman, D. D. (2007) Evaluation of assays for the measurement of bovine neutrophil reactive oxygen species. Vet. Immunol. Immunopathol. **115**, 107–125
38 Dikalov, S. I., Dikalova, A. E., Bikineyeva, A. T., Schmidt, H. H., Harrison, D. G. and Griendling, K. K. (2008) Distinct roles of Nox1 and Nox4 in basal and angiotensin II-stimulated superoxide and hydrogen peroxide production. Free Radical Biol. Med. **45**, 1340–1351
39 Nauseef, W. M. (2008) Biological roles for the NOX family NADPH oxidases. J. Biol. Chem. **283**, 16961–16965

40 Hunte, C. E., von Jagow, G. E. and Schagger, H. E. (2003) Membrane Protein Purification and Crystallization: A Practical Guide, 2nd Ed, Elsevier Science (USA), New York
41 Chen, Q. M. (2000) Replicative senescence and oxidant-induced premature senescence. Beyond the control of cell cycle checkpoints. Ann. N.Y. Acad. Sci. **908**, 111–125.
42 Hultdin, M., Gronlund, E., Norrback, K., Eriksson-Lindstrom, E., Just, T. and Roos, G. (1998) Telomere analysis by fluorescence *in situ* hybridization and flow cytometry. Nucleic Acids Res. **26**, 3651–3656
43 Voglauer, R., Chang, M. W., Dampier, B., Wieser, M., Baumann, K., Sterovsky, T., Schreiber, M., Katinger, H. and Grillari, J. (2006) SNEV overexpression extends the life span of human endothelial cells. Exp. Cell Res. **312**, 746–759
44 Nystrom, T. (2005) Role of oxidative carbonylation in protein quality control and senescence. EMBO J. **24**, 1311–1317
45 Bartek, J. and Lukas, J. (2007) DNA damage checkpoints: from initiation to recovery or adaptation. Curr. Opin. Cell Biol. **19**, 238–245
46 d'Adda di Fagagna, F. (2008) Living on a break: cellular senescence as a DNA-damage response. Nat. Rev. Cancer **8**, 512–522
47 Li, J. M. and Shah, A. M. (2002) Intracellular localization and preassembly of the NADPH oxidase complex in cultured endothelial cells. J. Biol. Chem. **277**, 19952–19960
48 Ushio-Fukai, M., Alexander, R. W., Akers, M. and Griendling, K. K. (1998) p38 mitogen-activated protein kinase is a critical component of the redox-sensitive signaling pathways activated by angiotensin II. Role in vascular smooth muscle cell hypertrophy. J. Biol. Chem. **273**, 15022–15029
49 Viedt, C., Soto, U., Krieger-Brauer, H. I., Fei, J., Elsing, C., Kubler, W. and Kreuzer, J. (2000) Differential activation of mitogen-activated protein kinases in smooth muscle cells by angiotensin II: involvement of $p22^{phox}$ and reactive oxygen species. Arterioscler. Thromb. Vasc. Biol. **20**, 940–948
50 Geiszt, M., Kopp, J. B., Varnai, P. and Leto, T. L. (2000) Identification of renox, an NAD(P)H oxidase in kidney. Proc. Natl. Acad. Sci. U.S.A. **97**, 8010–8014
51 Imanishi, T., Hano, T. and Nishio, I. (2005) Angiotensin II accelerates endothelial progenitor cell senescence through induction of oxidative stress. J. Hypertens. **23**, 97–104
52 Yao, E. H., Fukuda, N., Matsumoto, T., Kobayashi, N., Katakawa, M., Yamamoto, C., Tsunemi, A., Suzuki, R., Ueno, T. and Matsumoto, K. (2007) Losartan improves the impaired function of endothelial progenitor cells in hypertension via an antioxidant effect. Hypertens. Res. **30**, 1119–1128
53 Schilder, Y. D., Heiss, E. H., Schachner, D., Ziegler, J., Reznicek, G., Sorescu, D. and Dirsch, V. M. (2009) NADPH oxidases 1 and 4 mediate cellular senescence induced by resveratrol in human endothelial cells. Free Radical Biol. Med. **46**, 1598–1606

Received 5 May 2009/5 August 2009; accepted 14 August 2009
Published as BJ Immediate Publication 14 August 2009, doi:10.1042/BJ20090666

Biochem. J. (2009) **423**, 363–374 (Printed in Great Britain) doi:10.1042/BJ20090666

online data

SUPPLEMENTARY ONLINE DATA

The NADPH oxidase NOX4 restricts the replicative lifespan of human endothelial cells

Barbara LENER*†[1], Rafał KOZIEŁ*[1], Haymo PIRCHER*, Eveline HÜTTER*, Ruth GREUSSING*, Dietmar HERNDLER-BRANDSTETTER*, Martin HERMANN‡, Hermann UNTERLUGGAUER* and Pidder JANSEN-DÜRR*†[2]

*Institute for Biomedical Aging Research, Austrian Academy of Sciences, Rennweg 10, A-6020 Innsbruck, Austria, †Tyrolean Cancer Research Institute, Innrain 66, A-6020 Innsbruck, Austria, and ‡KMT Laboratory, Department of Visceral, Transplant and Thoracic Surgery, Center of Operative Medicine, Innsbruck Medical University, Innrain 66, A-6020 Innsbruck, Austria

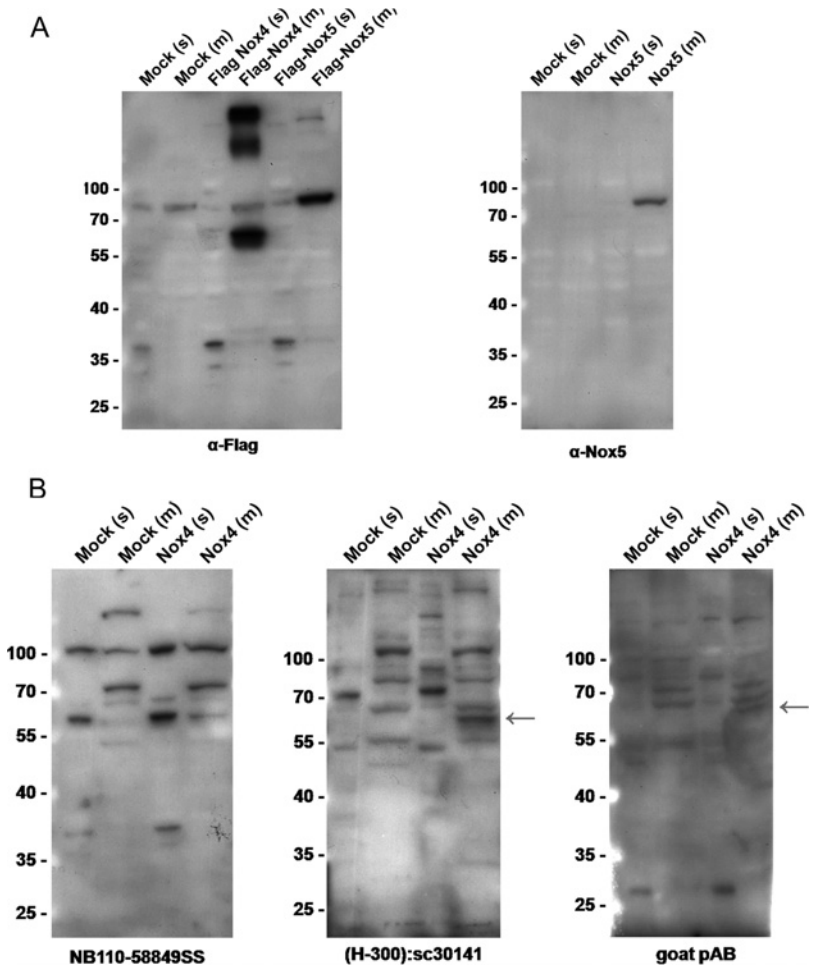

Figure S1 Extraction and expression of Nox4 in U-2OS cells

(**A**) Validation of lysis protocol. U-2OS osteosarcoma cells were transfected with expression vectors encoding Nox4, Nox5, FLAG–Nox4 and FLAG–Nox5, as indicated. Cells were lysed and separated in membrane (m) and soluble (s) protein fractions. Upon transfection of U-2OS cells with plasmids encoding either FLAG–Nox4 or FLAG–Nox5, specific bands of the expected size were detected in the membrane fraction using anti-FLAG antibodies (α-Flag, left panel). In case of FLAG–Nox4, one specific band corresponding to approx. 60 kDa was detected, which most likely refers to monomeric FLAG–Nox4. Two additional specific bands of higher molecular mass were present, probably representing FLAG–Nox4 protein that was only partially solubilized under the lysis conditions. In the case of FLAG–Nox5, a single band corresponding to approx. 70 kDa was specifically recognized by anti-FLAG antibodies, a result that could be reproduced by the application of Nox5 antibodies (α-Nox5, right panel). (**B**) Analysis of Nox4 overexpression by Western blot. U-2OS cells were transfected with Nox4 expression vector (Nox4) and empty vector (Mock), as indicated. Cells were treated as described for (**A**) and probed with three different antibodies to Nox4, as indicated. In addition to two commercially available antibodies, we used an affinity-purified goat antiserum that had been obtained against the C-terminal part of Nox4 after expression in *E. coli* and follow-up purification to homogeneity (anti-Nox4 NB110-58849SS; H. Pircher, unpublished work). Specific bands corresponding to overexpressed Nox4 (marked by an arrow) could be detected in the membrane fraction by anti-Nox4 (H-300):sc30141 and the affinity-purified goat antibody, whereas no specific band was detected by anti-Nox4 NB110-58849SS. Molecular mass in kDa is indicated to the left of each gel.

Received 5 May 2009/5 August 2009; accepted 14 August 2009
Published as BJ Immediate Publication 14 August 2009, doi:10.1042/BJ20090666

[1] These two authors contributed equally to this work
[2] To whom correspondence should be addressed (email p.jansen-duerr@oeaw.ac.at).